Inorg. Chem. **2009**, *48*, 2534−2540

Inorganic Chemistry

Article

Synthesis of Bis(phosphinoferrocenyl) Copper Complexes from Zwitterionic Quinonoid Ligands and Their Structural and Redox Properties[†]

Pierre Braunstein,*,[‡] Denis Bubrin,[§] and Biprajit Sarkar*,[‡],[§]

Laboratoire de Chimie de Coordination, Institut de Chimie (UMR 7177 CNRS), Université de Strasbourg, 4 rue Blaise Pascal, F-67070 Strasbourg Cédex, France, and Institut für Anorganische Chemie, Universität Stuttgart, Pfaffenwaldring 55, D-70550 Stuttgart, Germany

Received October 24, 2008

Reactions of *N,N′*-di-*n*-butyl-2-amino-5-alcoholate-1,4-benzoquinonemonoiminium **L^1**, or *N,N′*-diisopropyl-2-amino-5-alcoholate-1,4-benzoquinonemonoiminium **L^2** with [{(dppf)Cu}$_2$(μ−Cl)$_2$] (dppf = 1,1′-bis(diphenylphosphino)ferrocene) or [{(dispf)Cu}$_2$(μ−Cl)$_2$] (dispf = 1,1′-bis(diisopropylphosphino)ferrocene) led to the formation of the heterodinuclear complexes [(dppf)(Cu**L^1**$_{-H}$)] (**2**), [(dppf)(Cu**L^2**$_{-H}$)] (**3**), [(dispf)(Cu**L^1**$_{-H}$)] (**4**), and [(dispf)(Cu**L^2**$_{-H}$)] (**5**). The crystal structure of **L^2** was determined by X-ray diffraction and shows that the molecule exists in a $6\pi + 6\pi$ zwitterionic form, with two chemically connected but electronically nonconjugated π-subunits. The crystal structures of complexes **2**−**4** show a distorted tetrahedral coordination environment for the Cu(I) center and a more localized π-system for the ligands. Cyclic voltammetry on the ligands and complexes indicates various redox processes. The first oxidation of the complexes leads to an electron paramagnetic resonance supported formulation where the ligand radical is bound to Cu(I). UV−visible spectroscopy of the ligands and the complexes is also reported and discussed.

Introduction

The copper/quinone interactions play an important role in different areas of chemistry[1] and are relevant to current research areas as diverse as biochemical systems,[2−4] molecular devices,[5−7] and photochemical charge transfer.[8] The bis-chelating quinonoid ligand 2,5-dihydroxy-1,4-benzoquinone (**a**, Scheme 1) has been much used in coordination chemistry, and it has allowed the preparation of hundreds of metal complexes, including molecular boxes for supramolecular chemistry.[9]

Recently, such ligands have attracted much attention as spacers in polynuclear complexes because they combine metal-based and ligand-based redox activity.[10−13] The related ligands (**b**, Scheme 1) with a N, O, N, O donor set have also become popular as spacers for the study of metal−metal interactions[14,15] and the formation of magnetic materials[16] and in homogeneous catalysis.[17,18] In contrast, the ligands

Scheme 1

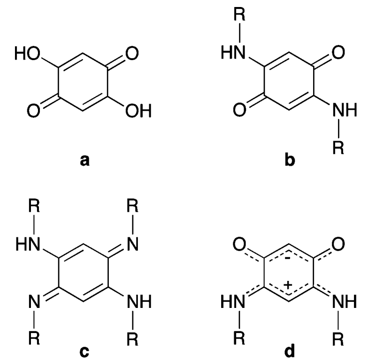

[†] Dedicated to Prof. Ingo-Peter Lorenz on the occasion of his 65th birthday, with our warmest congratulations and best wishes.

* To whom correspondence should be addressed. E-mail: braunstein@chimie.u-strasbg.fr.

[‡] Université de Strasbourg.

[§] Universität Stuttgart.

(1) Kaim, W. *Dalton Trans.* **2003**, 761.

(2) da Silva, G. F. Z.; Ming, L.-J. *Angew. Chem., Int. Ed.* **2007**, *46*, 3337.

(3) Decker, H.; Schweikardt, T.; Tuczek, F. *Angew. Chem., Int. Ed.* **2006**, *45*, 4546.

(4) Lee, Y.; Sayre, L. M. *J. Am. Chem. Soc.* **1995**, *117*, 3096.

(5) Pierpont, C. G.; Lange, C. W. *Prog. Inorg. Chem.* **1994**, *41*, 331.

(6) Pierpont, C. G. *Coord. Chem. Rev.* **2001**, *216−217*, 95.

(7) Hendrickson, D. N.; Pierpont, C. G. *Top. Curr. Chem.* **2004**, *234*, 63.

(8) Kunkely, H.; Vogler, A. *J. Photochem. Photobiol., A* **2002**, *147*, 149.

(9) Therrien, B.; Süss-Fink, G.; Govindaswamy, P.; Renfrew, A. K.; Dyson, P. J. *Angew. Chem., Int. Ed.* **2008**, *47*, 3773.

(10) Ward, M. D. *Inorg. Chem.* **1996**, *35*, 1712.

(11) Kitagawa, S.; Kawata, S. *Coord. Chem. Rev.* **2002**, *224*, 11.

(12) Leschke, M.; Melter, M.; Lang, H. *Inorg. Chim. Acta* **2003**, *350*, 114.

(13) Carbonera, C.; Dei, A.; Létard, J.-F.; Sangregorio, C.; Sorace, L. *Angew. Chem., Int. Ed.* **2004**, *43*, 3136.

(14) Kar, S.; Sarkar, B.; Ghumaan, S.; Janardanan, D.; van Slageren, J.; Fiedler, J.; Puranik, V. G.; Sunoj, R. B.; Kaim, W.; Lahiri, G. K. *Chem. Eur. J.* **2005**, *11*, 4901.

(15) Cotton, F. A.; Jin, J.-Y.; Li, Z.; Murillo, C. A.; Reibenspies, J. H. *Chem. Commun.* **2008**, 211.

10.1021/ic802042w CCC: $40.75

with N, N, N, N donor atoms (**c**, Scheme 1)[19] have been much less used in coordination chemistry,[20] with a few new examples appearing in recent years.[19,21−24]

Over the past few years our laboratory has developed a very efficient and facile access to zwitterionic *N*-substituted benzoquinonemonoimines (**d**, Scheme 1).[25,26] Following the synthesis of the first member of this unique family of molecules,[27,28] which are rare examples of potentially antiaromatic zwitterions being more stable than their canonical form and have therefore aroused the interest of numerous theoreticians,[28−32] we have developed a very general, straightforward, and "green" route to prepare such ligands.[25,26] Metalation of these ligands with various metal complex precursors has shown their potential in homogeneous catalysis[33] and supramolecular chemistry.[26] Furthermore, the possibility of including a donor atom into the R group of such ligands (**d**, Scheme 1) and the enhanced catalytic activity of the resulting metal complexes was also shown.[34] Recently, these ligands have been found to be exceptionally good facilitators of electronic communication between two quadruply bonded dimolybdenum units.[15]

Complexes of Cu(I) with *o*-quinonemonoimines are known in the literature.[35] In addition, the interactions of the O,O-chelating *o*-quinones (including the one-electron reduced *o*-semiquinone form) with Cu(I) have been studied in the context of valence tautomerism and their biological relevance.[36−38] To the best of our knowledge, there is only one Cu(I) complex reported so far with the ligands shown in Scheme 1, only with ligands of type **c**.[20] This complex, **1**, was formed through a metal-induced tautomerism of the *p*- to the *o*-quinone form associated with the migration of a proton from one nitrogen center to another.

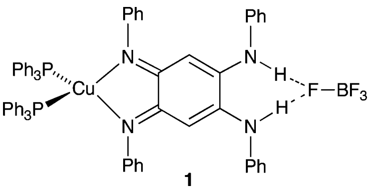

1

A similar proton migration was also observed with $W(CO)_4$ complexes of such ligands,[39] and these observations were consistent with earlier studies on the proton dynamics in azophenine.[40,41] Considering the rich potential of the zwitterionic ligands **d** (Scheme 1) in coordination and redox chemistry and the importance of Cu/quinone complexes in chemistry[5,6] and biochemistry,[2,3] we set out to react the ligands $\mathbf{L^1}$ and $\mathbf{L^2}$ (Scheme 1, **d** with R = *n*-butyl or *i*-propyl, respectively) with the diphosphine Cu(I) complexes $[\{(dppf)Cu\}_2(\mu{-}Cl)_2]$ (dppf = 1,1′-bis(diphenylphosphino)ferrocene) and $[\{(dispf)Cu\}_2(\mu{-}Cl)_2]$ (dispf = 1,1′-bis(diisopropyl phosphino)ferrocene), respectively. We have used dppf and dispf as ancillary ligands because their redox-active group and their chelation ability should provide additional stability to the resulting metal complexes.[42] In the following, results obtained from X-ray crystallography, cyclic voltammetry, electron paramagnetic resonance (EPR) spectroscopy, and ultraviolet−visible (UV−vis) spectroscopy on the ligands and the resulting heterodinuclear complexes will be discussed.

Results and Discussion

Ligand Synthesis. The ligand $\mathbf{L^2}$ was synthesized in a straightforward way from 4,6-diaminoresorcinol dihydrochloride and excess of isopropyl amine in water. This synthesis is similar to that reported earlier for $\mathbf{L^1}$ and related ligands.[25,26] The ligands were characterized by ^1H NMR spectroscopy, elemental analysis, and in the case of $\mathbf{L^2}$, by X-ray crystallography.

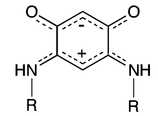

$\mathbf{L^1}$ R = *n*-butyl
$\mathbf{L^2}$ R = *i*-propyl

Crystal data and details of the structure determination are listed in Table 1. The structural parameters of $\mathbf{L^2}$ confirm its zwitterionic nature, with a fully delocalized π-system within each of the O1−C1−C2−C3−O2 and N1−C6−C5−C4−N2 moieties (Figure 1). The corresponding pairs of C−O, C−N, and C−C bond lengths are very similar (Table 2). The C1−C6 and C3−C4 distances of 1.538(2) and 1.533(2) Å, respectively, correspond clearly to single bonds and indicate a lack of conjugation between the two "6π halves" of the ligand which is thus best described as a zwitterionic $6\pi + 6\pi$ electron molecule.[26,28]

Synthesis of the Complexes. The precursor complex $[\{(dispf)Cu\}_2(\mu{-}Cl)_2]$ was synthesized from CuCl and dispf

---

(16) Margraf, G.; Kretz, T.; Fabrizi de Biani, F.; Laschi, F.; Losi, S.; Zanello, P.; Bats, J. W.; Wolf, B.; Langer, K. R.; Lang, M.; Prokofiev, A.; Assmus, W.; Lerner, H.-W.; Wagner, M. *Inorg. Chem.* **2006**, *45*, 1277.

(17) Zhang, D.; Jin, G.-X. *Organometallics* **2003**, *22*, 2851.

(18) Scheuermann, S.; Kretz, T.; Vitze, H.; Bats, J. W.; Bolte, M.; Lerner, H.-W.; Wagner, M. *Chem. Eur. J.* **2008**, *14*, 2590.

(19) Siri, O.; Braunstein, P.; Rohmer, M.-M.; Bénard, M.; Welter, R. *J. Am. Chem. Soc.* **2003**, *125*, 13793.

(20) (a) Rall, J.; Stange, A. F.; Hübler, K.; Kaim, W. *Angew. Chem., Int. Ed.* **1998**, *37*, 2681. (b) Braunstein, P.; Demessence, A.; Siri, O.; Taquet, J.-P. *C. R. Chim.* **2004**, *7*, 909.

(21) Frantz, S.; Rall, J.; Hartenbach, I.; Schleid, T.; Zalis, S.; Kaim, W. *Chem. Eur. J.* **2004**, *10*, 149.

(22) Siri, O.; Taquet, J.-P.; Collin, J.-P.; Rohmer, M.-M.; Bénard, M.; Braunstein, P. *Chem. Eur. J.* **2005**, *11*, 7247.

(23) Taquet, J.-P.; Siri, O.; Braunstein, P.; Welter, R. *Inorg. Chem.* **2006**, *45*, 4668.

(24) Siri, O.; Braunstein, P.; Taquet, J.-P.; Collin, J.-P.; Welter, R. *Dalton Trans.* **2007**, 1481.

(25) Yang, Q. Z.; Siri, O.; Braunstein, P. *Chem. Commun.* **2005**, 2660.

(26) Yang, Q. Z.; Siri, O.; Braunstein, P. *Chem. Eur. J.* **2005**, *11*, 7237.

(27) Siri, O.; Braunstein, P. *Chem. Commun.* **2002**, 208.

(28) Braunstein, P.; Siri, O.; Taquet, J.-P.; Rohmer, M.-M.; Bénard, M.; Welter, R. *J. Am. Chem. Soc.* **2003**, *125*, 12246.

(29) Sawicka, A.; Skurski, P.; Simons, J. *Chem. Phys. Lett.* **2002**, *362*, 527.

(30) Le, H. T.; Nam, P. C.; Dao, Y. L.; Veszpremi, T.; Nguyen, M. T. *Mol. Phys.* **2003**, *101*, 2347.

(31) Delaere, D.; Nam, P. C.; Nguyen, M. T. *Chem. Phys. Lett.* **2003**, *382*, 349.

(32) Haas, Y.; Zilberg, S. *J. Am. Chem. Soc.* **2004**, *126*, 8991.

(33) Taquet, J.-P.; Siri, O.; Braunstein, P.; Welter, R. *Inorg. Chem.* **2004**, *43*, 6944.

(34) Yang, Q. Z.; Kermagoret, A.; Agostinho, M.; Siri, O.; Braunstein, P. *Organometallics* **2006**, *25*, 5518.

(35) Speier, G.; Csihony, J.; Whalen, A. M.; Pierpont, C. G. *Inorg. Chim. Acta* **1996**, *245*, 1.

Table 1. Crystal Data and Details of the Structure Determination for $\mathbf{L}^2$ and **2**−**4**

crystal data	$\mathbf{L}^2$	**2**	**3**	**4**
formula	$C_{12}H_{18}N_2O_2$	$C_{48}H_{49}N_2CuFeO_2P_2$	$C_{46}H_{45}N_2CuFeO_2P_2$	$C_{36}H_{57}N_2CuFeO_2P_2$
formula weight (g·mol^{-1})	222.28	867.22	839.19	731.17
crystal system	orthorhombic	monoclinic	monoclinic	triclinic
space group	$P2_12_12_1$	$P2_1/n$	$P2_1/n$	$P\bar{1}$
a [Å]	5.7087(8)	11.344(4)	10.488(2)	11.5638(4)
b [Å]	14.096(2)	23.552(11)	23.362(4)	16.3723(7)
c [Å]	15.390(3)	15.910(7)	16.579(3)	20.7837(5)
α [deg]	90	90	90	92.505(2)
β [deg]	90	98.34(3)	98.600(17)	105.466(2)
γ [deg]	90	90	90	97.362(2)
V [Å^3]	1238.5(3)	4206(3)	4016.3(14)	3748.6(2)
Z	4	4	4	4
density (calcd) [g·cm^{-3}]	1.192	1.370	1.391	1.296
μ(Mo Kα) [mm^{-1}]	0.08	0.97	1.01	1.07
F(000)	480	1808	1752	1552
temperature (K)	173(2)	173(2)	173(2)	173(2)
θ min–max [deg]	1.96–27.98	2.01–26.00	1.52–26.00	2.35–26.00
data set [h; k; l]	0/7; −1/18; −1/20	−13/13; −6/29; −19/19	−3/12; −8/28; −20/20	−13/14; −20/16; −25/25
tot., unique data, R(int)	2003, 1938, 0.027	8672, 8247, 0.086	8854, 7883, 0.077	20834, 14654, 0.040
observed data [$I > 2\sigma(I)$]	1624	2528	3744	8449
No. reflns, No. params	1938, 160	8247, 478	7883, 491	14654, 815
R, wR$_2$, GOF [$I > 2\sigma(I)$]	0.0378, 0.0968, 0.995	0.0782, 0.1861, 0.714	0.0516, 0.1050, 0.737	0.0683, 0.1166, 1.039

by a procedure similar to that already reported for [{(dppf)Cu}$_2$(μ−Cl)$_2$].[43] This compound was characterized by ^{1}H and ^{31}P{^{1}H} NMR spectroscopy and elemental analysis. The heterodinuclear bis(phosphinoferrocenyl) copper complexes **2**−**5** were prepared as outlined in Scheme 2. Monodeprotonation of $\mathbf{L}^1$ or $\mathbf{L}^2$ with equimolar amounts of KO^{t}Bu followed by reaction with [{(dppf)Cu}$_2$(μ−Cl)$_2$] or [{(dispf)Cu}$_2$(μ−Cl)$_2$] afforded the products in high yields. These complexes were characterized by ^{1}H and ^{31}P{^{1}H} NMR spectroscopy and elemental analysis. Metalation of $\mathbf{L}^1$ and $\mathbf{L}^2$ results in the localization of their π-system (see discussion of crystal structures below). Slow diffusion of *n*-hexane into a dichloromethane solution of **2**−**4** afforded crystals suitable for X-ray diffraction. Crystal data and details of the structure determination are listed in Table 1. Selected bond lengths and angles are given in Tables 2 and 3, respectively.

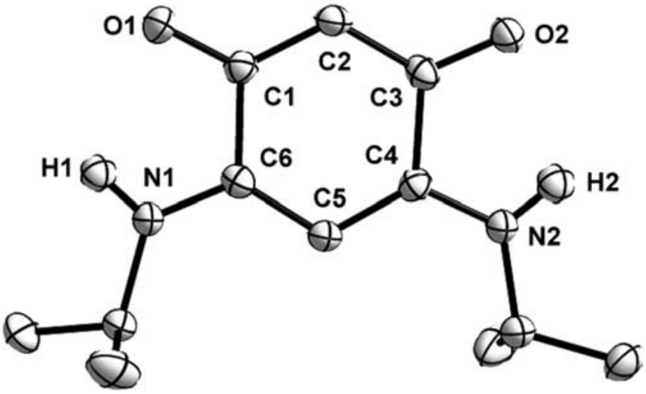

Figure 1. Oak Ridge thermal ellipsoid plot (ORTEP) view of $\mathbf{L}^2$. Thermal ellipsoids enclose 50% of the electron density.

Table 2. Comparison among Selected Interatomic Distances (Å) in $\mathbf{L}^2$, **2** and **3**, and One of the Two Molecules of **2** and **3**, and One of the Two Molecules of 4

	$\mathbf{L}^2$	**2**	**3**	**4**
Cu−O1		2.084(5)	2.084(3)	2.113(3)
Cu−N1		2.001(8)	2.062(4)	2.037(3)
Cu−P1		2.261(2)	2.273(2)	2.269(1)
Cu−P2		2.245(3)	2.264(1)	2.247(1)
C1−C2	1.398(2)	1.39(1)	1.385(7)	1.387(5)
C1−C6	1.538(2)	1.50(1)	1.520(7)	1.514(6)
C2−C3	1.401(2)	1.42(1)	1.393(7)	1.397(5)
C3−C4	1.533(2)	1.50(1)	1.534(7)	1.502(6)
C4−C5	1.393(2)	1.34(1)	1.369(6)	1.376(5)
C5−C6	1.395(2)	1.43(1)	1.423(6)	1.421(5)
C1−O1	1.251(2)	1.284(9)	1.292(6)	1.272(5)
C6−N1	1.321(2)	1.30(1)	1.309(6)	1.313(5)
C3−O2	1.252(2)	1.243(8)	1.252(5)	1.254(4)
C4−N2	1.322(2)	1.35(1)	1.342(6)	1.330(5)

The copper center in complexes **2**−**4** (Figures 2−4) adopts a distorted tetrahedral geometry as seen from the O1−Cu−P1 and N1−Cu−P2 angles (103.1(2)° and 116.6(2)° for **2**, 107.8(1)° and 120.3(1)° for **3**, and 104.6(1)° and 115.4(1)° for **4**, respectively, Table 3). In all three compounds, the Cu−O1 and Cu−P1 distances are slightly longer than the Cu−N1 and Cu−P2 distances, and accordingly, the O1−Cu−P1 angle is smaller than the N1−Cu−P2 angle (Table 3).

In complexes **2**−**4**, examination of the respective bond distances within the N1−C6−C5−C4−N2 moiety reveals an alternation of single and double bonds,[44] which is consistent with two conjugated but localized π-systems (Table 2). This result is in agreement with the localization of the π-system found in other metal complexes with such ligands.[28,33] In keeping with related crystallographic structures previously described,[26,28,33] the C1−C6 and C3−C4 distances of 1.50(1) Å for **2**, 1.520(7) Å and 1.534(7) Å for

---

(36) Rall, J.; Kaim, W. *J. Chem. Soc., Faraday Trans.* **1994**, *90*, 2905.
(37) Rall, J.; Wanner, M.; Albrecht, M.; Hornung, F. M.; Kaim, W. *Chem. Eur. J.* **1999**, *5*, 2802.
(38) Ye, S.; Sarkar, B.; Niemeyer, M.; Kaim, W. *Eur. J. Inorg. Chem.* **2005**, 4735.
(39) Braunstein, P.; Demessence, A.; Siri, O.; Taquet, J.-P. *C. R. Chim.* **2004**, *7*, 909.
(40) Rumpel, H.; Limbach, H.-H. *J. Am. Chem. Soc.* **1989**, *111*, 5429.
(41) Rumpel, H.; Limbach, H.-H.; Zachmann, G. *J. Phys. Chem.* **1989**, *93*, 1812.
(42) Femoni, C.; Iapalucci, M. C.; Longoni, G.; Svensson, P. H.; Zanello, P.; Fabrizi de Biani, F. *Chem. Eur.—J.* **2004**, *10*, 2318.
(43) Diez, J.; Gamasa, M. P.; Gimeno, J.; Aguirre, A.; García-Granda, S. *Organometallics* **1999**, *18*, 662.
(44) van Bolhuis, F.; Kiers, C. T. *Acta Crystallogr., Sect. B: Struct. Sci.* **1978**, *34*, 1015.

Scheme 2

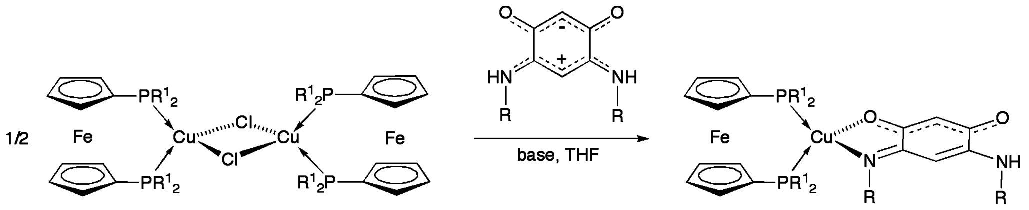

R^1 = phenyl or isopropyl

2 R^1 = phenyl, R = *n*-butyl
3 R^1 = phenyl, R = *i*-propyl
4 R^1 = *i*-propyl, R = *n*-butyl
5 R^1 = *i*-propyl, R = *i*-propyl

Table 3. Selected Bond Angles (deg) in **2** and **3** and One of the Two Molecules of **4**

	2	**3**	**4**
O1−Cu−N1	78.9(3)	79.57(14)	79.20(12)
O1−Cu−P1	103.1(2)	107.8(1)	104.59(9)
O1−Cu−P2	118.9(2)	110.0(1)	107.94(9)
N1−Cu−P2	116.6(2)	120.3(1)	115.4(1)
N1−Cu−P1	122.3(2)	122.8(1)	125.8(1)
P1−Cu−P2	112.02(9)	110.19(5)	114.38(5)

3, and 1.514(6) Å and 1.502(6) Å for **4**, respectively, correspond to single bonds and indicate the lack of conjugation between the two 6π-subunits. As reported earlier, monodeprotonation of ligands of the type $\mathbf{L^1}$ or $\mathbf{L^2}$ leads to monometallic complexes where the π-systems become more localized.[33,39] The only Cu(I) complex which was earlier reported in the literature[20] with the N, N, N, N-type ligand **c** (Scheme 1), **1**, has a different bonding pattern than the complexes described here. In **1**, the chelating N-donor centers have to adopt a *o*-quinonediimine form because of proton migration, whereas such a situation is not necessary for complexes **2**−**5** because the ligands $\mathbf{L^1}$ and $\mathbf{L^2}$ in these complexes exist in a monodeprotonated form.

Electrochemistry, UV−Vis Spectroscopy, and EPR Spectroscopy. Ligands $\mathbf{L^1}$ and $\mathbf{L^2}$ show one irreversible oxidation and two irreversible reduction waves in CH_2Cl_2/0.1 M Bu_4NPF_6. The reversibility of the cyclic voltammetric responses did not improve even at lower temperatures or with higher scan rates. The potentials of the redox processes are almost identical for both ligands (Table 4).

Complexes **2**−**5**display a reversible oxidation at 233 K in CH_2Cl_2/0.1 M Bu_4NPF_6. They also show a further irreversible oxidation and an irreversible reduction (Figure 5). All of the processes, including the first oxidation, are irreversible at room temperature. Compared to the free ligands, the potentials of the complexes are all shifted to more negative values (Table 4), confirming the π-donor character of the Cu(I) center. The effect of the N-substituents (*n*-butyl vs *i*-propyl) on the redox potentials of the complexes is marginal. On comparing complexes with the same ligands but different substituents on the phosphorus atoms (**2** and **4** for example), one notices a fairly large shift of the redox potentials. The first oxidation process for **4** and **5**, with *i*-propyl substituents on the phosphorus atoms, occurs at −0.09 and −0.03 V, respectively, whereas the same process for **2** and **3**, with phenyl substituents on the phosphorus atoms, occurs at 0.32 and 0.35 V, respectively. This shift can be explained by the superior donor properties of the *i*-propyl group compared to the phenyl group. A similar shift of all other redox processes to more negative potentials is also observed on going from **4** or **5** to **2** or **3** (Table 4).

The first oxidation as well as the reduction processes in the complexes are centered on ligand $\mathbf{L^1}$ or $\mathbf{L^2}$ (see EPR section below). The second oxidation is tentatively assigned to the oxidation of the ferrocene center in the complexes, by analogy with data for other Cu(I) complexes with the dppf ligand.[45] The second reduction wave observed for the ligands $\mathbf{L^1}$ or $\mathbf{L^2}$ is not seen in the complexes, probably because it lies outside the potential window of the solvent.

In the UV−vis spectrum of $\mathbf{L^1}$ or $\mathbf{L^2}$, two main bands are observed at around 350 and 330 nm, with high molar extinction coefficients (Figure 6, Table 5). Such bands have been previously observed for a related ligand.[28] The first band is assigned to a $\pi \rightarrow \pi^*$ transition and the second one to a vibrational excitation on top of the electronic transition.[29] The complexes also display the intraligand bands observed for the free ligands. In addition, all the complexes exhibit a band around 420 nm (Figure 6). This transition is due to a metal-to-ligand charge transfer (MLCT). The position as well as the intensity of the bands is very similar for all the complexes (Table 5).

The electrochemically generated one-electron oxidized form of the complexes shows an EPR signal at 233 K with *g* values around 2.03 (Figure 7, Table 6). The spectra could be simulated with ^{14}N ($I = 1$) couplings of around 6 G and $^{63,65}Cu$ ($I = 3/2$) couplings of around 11 G (Table 6). Attempts to simulate the EPR spectrum by using two different N atoms led to the same best fit as when considering one N atom, probably because of the poor spectral resolution due to the need to record the EPR spectrum at 233 K. The *g* value as well as the hyperfine coupling constants point to a species with a radical ligand bound to the Cu(I) center, by analogy with other complexes which have a radical ligand bound to Cu(I).[46] Even though there is a non-negligible contribution of the Cu center to the singly occupied molecular orbital (SOMO), the unpaired electron clearly is predominantly located at the ligand, leading to a formulation $[(\mathrm{dispf})\mathrm{Cu^I}(\mathbf{L^{1\bullet}})]^+$ for $\mathbf{4}^+$ and similarly for the other complexes.

---

(45) Roy, S.; Sieger, M.; Singh, P.; Niemeyer, M.; Fiedler, J.; Duboc, C.; Kaim, W. *Inorg. Chim. Acta* **2008**, *361*, 1699.

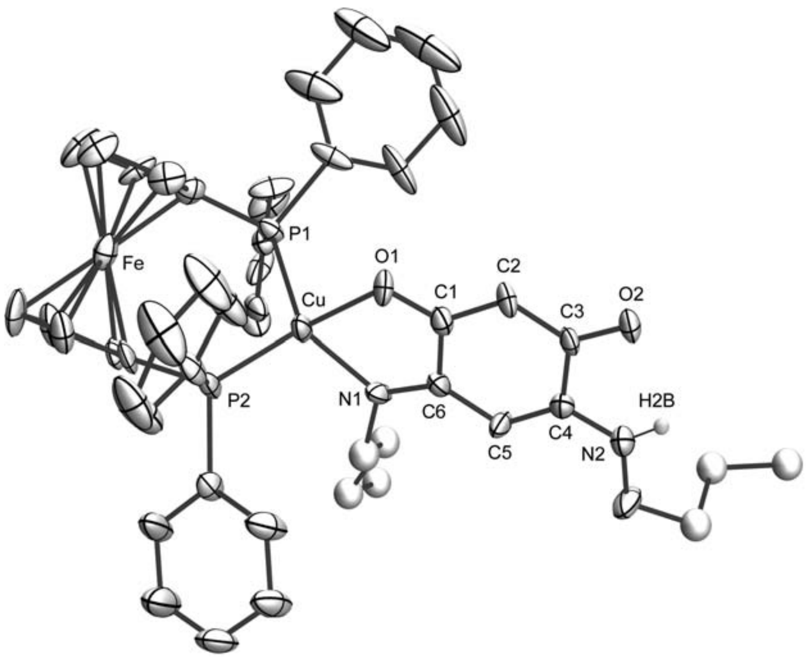

Figure 2. ORTEP view of **2**. Thermal ellipsoids enclose 30% of the electron density. Isotropically refined atoms are depicted as white spheres with an arbitrary radius.

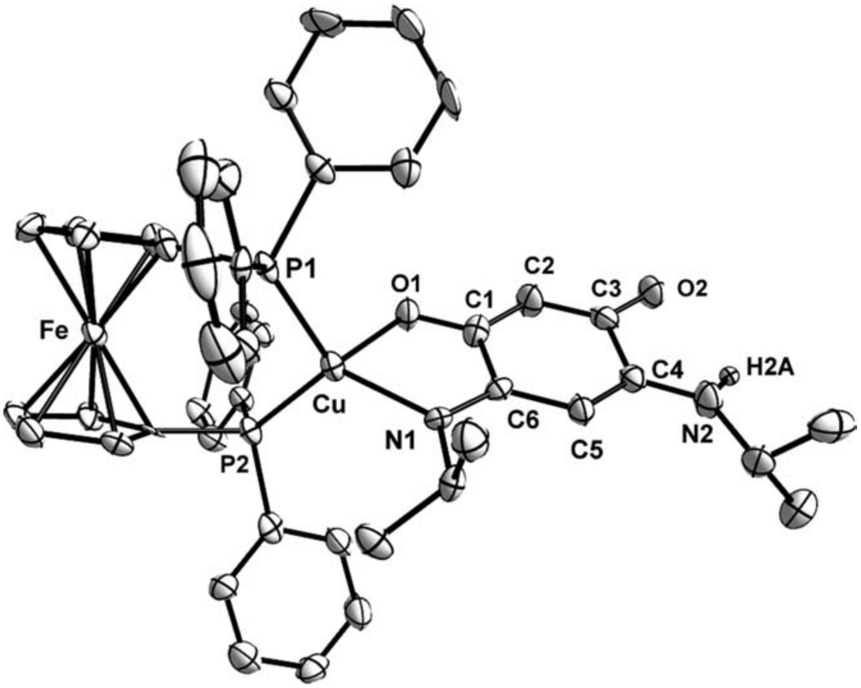

Figure 3. ORTEP view of **3**. Thermal ellipsoids enclose 50% of the electron density.

Conclusion

The ligands $\mathbf{L^1}$ and $\mathbf{L^2}$, synthesized from 4,6-diaminoresorcinol dihydrochloride and the respective primary amine, were reacted with the Cu(I) complex $[\{(\mathrm{dppf})\mathrm{Cu}\}_2(\mu{-}\mathrm{Cl})_2]$ or $[\{(\mathrm{dispf})\mathrm{Cu}\}_2(\mu{-}\mathrm{Cl})_2]$, and the heterodinuclear, bis(diphenylphosphino)ferrocene copper complexes **2**−**5** were obtained in good yields. Whereas the π-system of the free ligands is delocalized over the upper and lower half of the molecules, the complexes display increased bond localization. Cyclic voltammetry of the complexes show ligand- and ferrocene-centered oxidations and a ligand-centered reduction. EPR spectroscopy of the one-electron oxidized form of the ligands shows signals typical of a ligand radical bound to a Cu(I) center. In view of the differences in the ligand bonding patterns of complex **1**[20] compared to our complexes, it will be interesting to study the reactions of our ligands with Cu(I) precursors in the absence of a base. Further studies are in progress.

Experimental Section

General Considerations. The ligands were synthesized under normal atmospheric conditions using reagent grade solvents. For the metal complexes, all manipulations were carried out using Schlenk techniques under an argon atmosphere. The solvents used for metal complex synthesis were dried and distilled under argon

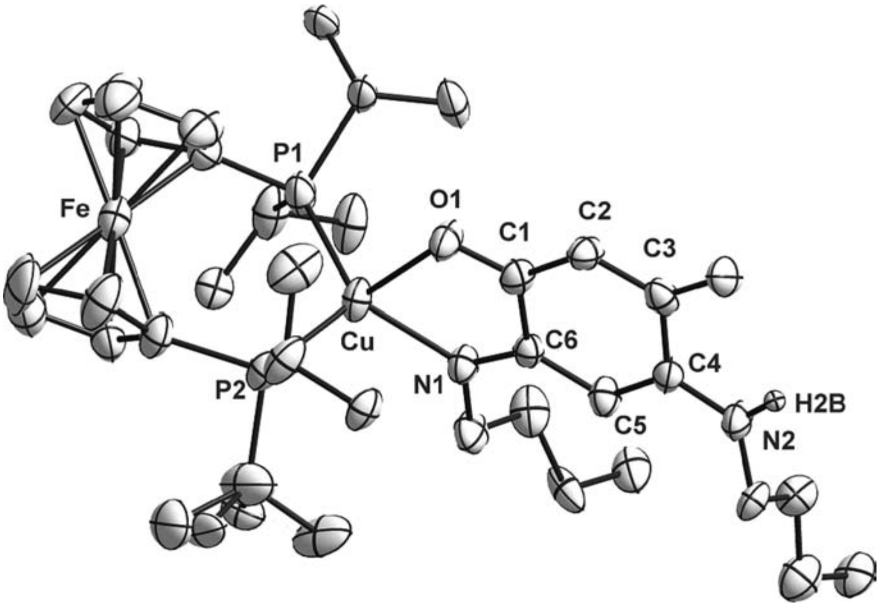

Figure 4. ORTEP view of **4**. The unit cell contains two independent but very similar molecules. Thermal ellipsoids enclose 50% of the electron density. The isopropyl group attached to P2 shows disorder.

Table 4. Redox Potentials of Ligands and Complexes[a]

compound	$E_{1/2}$ (ox1)	$E_{pa}{}^{b}$ (ox2)	$E_{pc}{}^{c}$ (red1)	$E_{pc}{}^{c}$ (red2)
$\mathbf{L^1}$	0.91[b]	n.o.[d]	−1.64	−2.24
$\mathbf{L^2}$	0.89[b]	n.o.	−1.62	−2.19
2	0.32	0.70	−1.99	n.o.
3	0.35	0.68	−1.92	n.o.
4	−0.09	0.42	−2.43	n.o.
5	−0.03	0.44	−2.46	n.o.

[a] Electrochemical potentials from cyclic voltammetry in CH_2Cl_2/0.1 M $(Bu_4N)PF_6$ at 233 K. The Fc^0/Fc^+ couple was used as an internal standard. [b] Anodic peak potential for irreversible oxidation. [c] Cathodic peak potential for irreversible reduction. [d] n.o. = not observed.

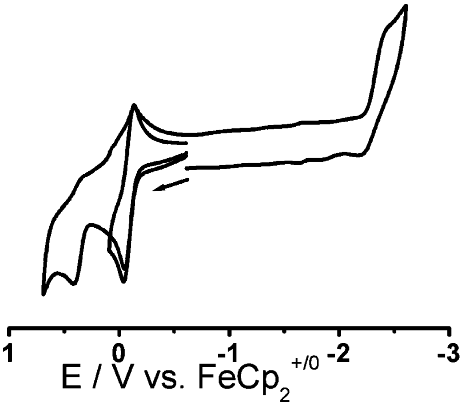

Figure 5. Cyclic voltammogram of **4** in CH_2Cl_2/0.1 M Bu_4NPF_6 at 233 K. Scan rate = 100 mV/s. The Fc^0/Fc^+ couple was used as an internal standard.

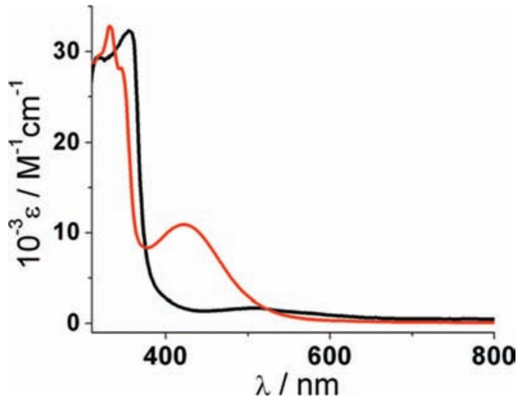

Figure 6. UV−vis spectra of $\mathbf{L^2}$ (black) and **3** (red) in CH_2Cl_2.

Table 5. UV−Vis Data of Ligands and Complexes in CH_2Cl_2

compound	λ (ε)[a]
$\mathbf{L^1}$	332 (29100), 351 (32400), 515sh
$\mathbf{L^2}$	336 (29400), 356 (32200), 515sh
2	330 (32400), 344sh, 422 (10900)
3	332 (32900), 345sh, 424 (11000)
4	332 (32500), 348sh, 426 (11200)
5	334 (32700), 347sh, 420 (10800)

[a] Wavelength in nanometers; molar extinction coefficient in $M^{-1}cm^{-1}$.

and degassed by common techniques prior to use. 4,6-Diaminoresorcinol dihydrochloride was purchased from Acros, CuCl and 1,1′-bis(diisopropylphosphino)ferrocene from Strem, and 1,1′-bis(diphenylphosphino) ferrocene from Alfa Aesar. The complex $[\{(dppf)Cu\}_2(\mu{-}Cl)_2]$[43] and the ligand $\mathbf{L^1}$ were prepared according to reported procedures.[25,26]

Instrumentation. The ^1H and $^{31}P\{^1H\}$ NMR spectra were recorded at 250.13 and 101.26 MHz, respectively, on a Brucker AC250 instrument. EPR spectra in the X-band were recorded with a Bruker System EMX. UV−vis near-infrared (NIR) absorption spectra were recorded on a Shimadzu UV 3101 PC spectrophotometer. Cyclic voltammetry was carried out in 0.1 M Bu_4NPF_6 solution using a three-electrode configuration (glassy carbon working electrode, Pt counter electrode, Ag wire as pseudoreference) and a PAR 273 potentiostat and function generator. The ferrocene/ferrocenium (Fc/Fc^+) couple served as internal reference. Elemental analyses were performed with a Perkin-Elmer Analyzer 240.

Synthesis of *N,N′*-Diisopropyl-2-amino-5-alcoholate-1,4-benzoquinonemono iminium ($\mathbf{L^2}$). 4,6-Diaminoresorcinol dihydrochloride (0.500 g, 2.35 mmol) was dissolved in water (7 mL), and an excess of isopropylamine (7 equiv) was added dropwise to this solution. The solution was stirred under air for 90 min. The purple precipitate thus formed was filtered, washed with cold water, and dried in air. Yield: 0.365 g (70%). ^1H NMR ($CDCl_3$, 298 K) δ: 1.34 (d, ^3J = 6.5 Hz, 12H, $CH_3{-}CH{-}NH$), 3.84 (sept., 2H, $CH_3{-}CH{-}NH$), 5.12

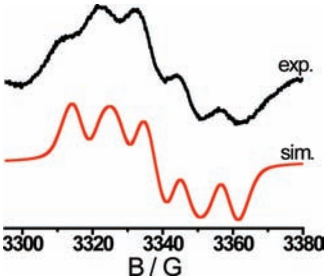

Figure 7. X-band EPR spectrum of electrochemically generated $\mathbf{4}^{\bullet+}$ in CH_2Cl_2/0.1 M Bu_4NPF_6 at 233 K (black = experimental, red = simulated).

Table 6. X-Band EPR Data of the Electrochemically Generated First Oxidized Form of the Complexes at 233 K in CH_2Cl_2/0.1 M $(Bu_4N)PF_6$

compound	*g*	*a* (N)[a]	*a* (Cu)[a]
$\mathbf{2}^{\bullet+}$	2.0315	6	10.8
$\mathbf{3}^{\bullet+}$	2.0320	5.8	11.3
$\mathbf{4}^{\bullet+}$	2.0290	6	11
$\mathbf{5}^{\bullet+}$	2.0282	6.3	11.2

[a] Hyperfine coupling constants in gauss obtained from simulation.

(s, 1H, N−C−C*H*), 5.45 (s, 1H, O−C−C*H*), 8.09 (s, br, 2H, N*H*). Anal. Calcd for $C_{12}H_{18}N_2O_2$: C, 64.84; H, 8.16; N, 12.60. Found: C, 64.65; H, 8.18; N, 12.47%.

Synthesis of [{(dispf)Cu}$_2$(μ−Cl)$_2$]. This compound was synthesized by a procedure identical to that reported for [{(dppf)Cu}$_2$(μ−Cl)$_2$] by using dispf instead of dppf.[1] Yield: 90%. ^{1}H NMR ($CDCl_3$, 298 K) δ: 1.27 (m, 48H, $\mathrm{C}H_3$), 2.22 (m, br, 8H, C*H*), 4.26 (s, br, 8H, ferrocene ring H), 4.39 (t, br, 8H, ferrocene ring H). ^{31}P{^{1}H} NMR ($CDCl_3$, 298 K) δ: −1.5. Anal. Calcd for $C_{44}H_{72}Cl_2Cu_2Fe_2P_4$: C, 51.08; H, 7.01. Found: C, 50.95; H, 7.21%.

Synthesis of [(dppf)Cu(L^1)] (2). To solid KO^{t}Bu (0.0112 g, 0.10 mmol) in a Schlenk flask was added **L^1** (0.025 g, 0.10 mmol) and tetrahydrofuran (10 mL). The color changed immediately from purple to orange. The solution was stirred overnight at room temperature under an argon atmosphere, and then the solvent was removed under vacuum. Then solid [{(dppf)Cu}$_2$(μ−Cl)$_2$] (0.0653 g, 0.05 mmol) and dichloromethane (15 mL) were added. The color changed immediately to red. The solution was stirred at room temperature for 4 h. It was then filtered over Celite to remove KCl. The volume of the solution was reduced by removing dichloromethane under reduced pressure. Finally, a four-fold excess of *n*-hexane was added to the solution which was left overnight at 4 °C. The red crystalline material which precipitated was filtered and washed with *n*-hexane. Yield: 0.035 g (85%). ^{1}H NMR ($CDCl_3$, 298 K) δ: 0.63 (t, ^3J = 7.3 Hz, 3H, $\mathrm{C}H_3$−CH_2−CH_2−CH_2−NH), 0.93 (t, ^3J = 7.3 Hz, 3H, $\mathrm{C}H_3$−CH_2−CH_2−CH_2−N), 1.02−1.72 (m, 8H, CH_3−$\mathrm{C}H_2$−$\mathrm{C}H_2$−CH_2), 3.09 (m, 2H, CH_3−CH_2−CH_2−$\mathrm{C}H_2$−NH), 3.35 (m, 2H, m, 2H, CH_3−CH_2−CH_2−$\mathrm{C}H_2$−N), 4.26 (s, br, 4H, ferrocene ring H), 4.33 (s, br, 4H, ferrocene ring H), 5.16 (s, 1H, N−C−C*H*), 5.65 (s, 1H, O−C−C*H*), 6.32 (t, br, 1H, N*H*), 7.20−7.55 (m, 20H, phenyl H). ^{31}P{^{1}H} NMR ($CDCl_3$, 298 K) δ: −15.3. Anal. Calcd for $C_{48}H_{49}N_2CuFeO_2P_2$: C, 66.48; H, 5.69; N, 3.23. Found: C, 66.25; H, 5.73; N, 3.38%.

Synthesis of [(dppf)Cu(L^2)] (3). This compound was synthesized similarly to [(dppf)Cu(**L^1**)] but using **L^2** instead of **L^1**. Yield: 80%. ^{1}H NMR ($CDCl_3$, 298 K) δ: 0.86 (d, ^3J = 6.4 Hz, 6H, $\mathrm{C}H_3$−CH−NH), 1.23 (d, ^3J = 6.5 Hz, 6H, $\mathrm{C}H_3$−CH−N), 3.55 (m, 1H, CH_3−C*H*−NH), 3.81 (m, 1H, CH_3−C*H*−N), 4.34 (d, br, 4H, ferrocene ring H), 4.36 (d, br, 4H, ferrocene ring H), 5.18 (s, 1H, N−C−C*H*), 5.64 (s, 1H, O−C−C*H*), 6.24 (d, br, 1H, N*H*), 7.25−7.52 (m, 20H, phenyl H). ^{31}P{^{1}H} NMR ($CDCl_3$, 298 K) δ: −16.2. Anal. Calcd for $C_{46}H_{45}N_2CuFeO_2P_2$: C, 65.84; H, 5.40; N, 3.34. Found: C, 65.51; H, 5.61; N, 3.19%.

Synthesis of [(dispf)Cu(L^1)] (4). This compound was synthesized similarly to [(dppf)Cu(**L^1**)] by using [{(dispf)Cu}$_2$(μ−Cl)$_2$] and **L**^{1}. Yield: 75%. ^{1}H NMR ($CDCl_3$, 298 K) δ: 0.94 (t, ^3J = 7.3 Hz, 3H, $\mathrm{C}H_3$−CH_2−CH_2−CH_2−NH), 0.99 (t, ^3J = 7.4 Hz, 3H, $\mathrm{C}H_3$−CH_2−CH_2−CH_2−N), 1.07 (dd, $^3J_{HH}$ = 7.1 Hz, $^3J_{PH}$ = 14.3 Hz, 12H, P−CH−$\mathrm{C}H_3$), 1.20 (dd, $^3J_{HH}$ = 7.1 Hz, $^3J_{PH}$ = 14.7 Hz, 12H, P−CH−$\mathrm{C}H_3$), 1.37−1.85 (m, 8H, CH_3−$\mathrm{C}H_2$−$\mathrm{C}H_2$−CH_2), 2.07 (m, 4H, P−C*H*−CH_3), 3.11 (m, 2H, CH_3−CH_2−CH_2−$\mathrm{C}H_2$−NH), 3.78 (m, 2H, CH_3−CH_2−CH_2−$\mathrm{C}H_2$−N), 4.36 (m, br, 8H, ferrocene ring H), 5.20 (s, 1H, N−C−C*H*), 5.61 (s, 1H, O−C−C*H*), 6.32 (t, br, 1H, N*H*). ^{31}P{^{1}H} NMR ($CDCl_3$, 298 K) δ: −1.0. Anal. Calcd for $C_{36}H_{57}N_2CuFeO_2P_2$: C, 59.13; H, 7.86; N, 3.83. Found: C, 59.28; H, 7.63; N, 3.95%.

Synthesis of [(dispf)Cu(L^2)] (5). This compound was synthesized similarly to [(dppf)Cu(**L^1**)] by using [{(dispf)Cu}$_2$(μ−Cl)$_2$] and **L^2**. Yield: 70%. ^{1}H NMR ($CDCl_3$, 298 K) δ: 1.06 (dd, $^3J_{HH}$ = 7.1 Hz, $^3J_{PH}$ = 14.0 Hz, 12H, P−CH−$\mathrm{C}H_3$), 1.16 (dd, $^3J_{HH}$ = 7.1 Hz, $^3J_{PH}$ = 14.3 Hz, 12H, P−CH−$\mathrm{C}H_3$), 1.25 (d, ^3J = 6.5 Hz, 6H, $\mathrm{C}H_3$−CH−NH), 1.41 (d, ^3J = 6.4 Hz, 6H, $\mathrm{C}H_3$−CH−N), 2.10 (m, 4H, P−C*H*−CH_3), 3.59 (m, 1H, CH_3−C*H*−NH), 4.12 (m, 1H, CH_3−C*H*−N), 4.34 (t, br, 4H, ferrocene ring H), 4.48 (s, br, 4H, ferrocene ring H), 5.26 (s, 1H, N−C−C*H*), 5.59 (s, 1H, O−C−C*H*), 6.26 (d, br, 1H, N*H*). ^{31}P{^{1}H} NMR ($CDCl_3$, 298 K) δ: −1.4. Anal. Calcd for $C_{34}H_{53}N_2CuFeO_2P_2$: C, 58.08; H, 7.60; N, 3.98. Found: C, 57.91; H, 7.70; N, 4.02%.

Crystal Structure Determination. Single crystals were grown by layering a dichloromethane solution of the compound with *n*-hexane at room temperature (**L^2**) or at 4 °C (**2**−**4**). A suitable crystal was selected under a layer of viscous hydrocarbon oil, attached to a glass fiber, and instantly placed in a low-temperature N_2 stream. Except for **4**, the X-ray intensity data were collected at 173 K using a Siemens P4 diffractometer. For **4**, the intensity data were collected at 173(2) K on a Kappa CCD diffractometer (graphite monochromated Mo-Kα radiation, λ = 0.71073 Å). Calculations were performed with the SHELXTL PC 5.03[47] and SHELXL-97 program[48] system installed on a local PC. The structures were solved by direct methods and refined on F_o^2 by full-matrix least-squares refinement. Unless otherwise stated, anisotropic thermal parameters were included for all non-hydrogen atoms.

Acknowledgment. We are grateful to the Ministère de la Recherche (Paris) for a postdoctoral grant to B.S. and to the CNRS and the ANR (07-BLAN-0274-04) for funding. B.S. is also indebted to the Landesstiftung Baden-Württemberg for financial support through the Eliteprogramme for Postdocs and to Kathrin Schellmann for experimental help. We thank Dr. R. Pattacini for crystal structure determination of **4**.

Supporting Information Available: Crystallographic data for all structures in this paper in CIF format. This material is available free of charge via the Internet at http://pubs.acs.org. Files have been deposited with the Cambridge Crystallographic Data Centre, CCDC 705553−705556. Copies of this information may be obtained free of charge from The Director, CCDC, 12 Union Road, Cambridge CB2 1EZ, U.K. (fax, +44-1223-336033; e-mail, deposit@ccdc.cam.ac.uk; online, http://www.ccdc.cam.ac.uk).

IC802042W

---

(46) Schwach, M.; Hausen, H.-D.; Kaim, W. *Chem. Eur. J.* **1996**, *2*, 446.
(47) *SHELXTL PC 5.03*; Siemens Analytical X-Ray Instruments Inc.: Madison, WI, 1994.
(48) Sheldrick, G. M. *Program for Crystal Structure Solution and Refinement*; Universität Göttingen: Göttingen, 1997.